# Wear comparison of critical dimension-atomic force microscopy tips

**Ndubuisi G. Orji,[a] Ronald G. Dixson,[a] Ernesto Lopez,[b] Bernd Irmer[c]**
[a]National Institute of Standards and Technology, Gaithersburg, MD 20850, USA
[b]nanotools USA LLC, Henderson, NV 89052, USA
[c]nanotools GmbH, Munich, D-80469, Germany

**Abstract**

Nanoscale wear affects the performance of atomic force microscopy (AFM)-based measurements for all applications including process control measurements and nanoelectronics characterization. As such, methods to prevent or reduce AFM tip wear is an area of active research. However, most prior work has been on conventional AFMs rather than critical dimension AFM (CD-AFM). Hence, less is known about CD-AFM tip-wear. Given that tip-wear directly affects the accuracy of dimensional measurements, a basic understanding of CD-AFM tip wear is needed. Toward this goal, we evaluated the wear performance of electron beam deposited CD-AFM tips. Using a continuous scanning strategy, we evaluated the overall wear rate and tip lifetime and compared these with those of silicon-based CD-AFM tips. Our data show improved tip lifetime of as much as a factor of five and reduced wear rates of more than 17 times. Such improvements in wear rate means less measurement variability and lower cost.

Keywords: tip wear, nanometrology, diamond like carbon, electron beam deposition, critical dimension atomic force microscopy.

## 1. Introduction

Atomic force microscopy (AFM) play key roles in integrated circuit metrology[1,2] by providing accurate measurements for process control and failure analysis, including linewidth and sidewall angle measurements[2-5]. Since AFM information comes from the interaction of the tip and surface forces, tip changes of any type including wear and brakeage, directly introduce errors to the results. Tip-wear limits the performance of AFM-based metrology[6], fabrication, and affects other methods that depend on AFM for calibration[7-10] because such errors propagate to all underlying measurements. Hence, tips that can be used for an extended period of time with little change in structural and functional properties are desirable, both from a reliability and cost point of view. While tips that could be used indefinitely without wear are unavailable, models of nanoscale wear, accurate tip-wear analysis, wear resistant probes and coatings, and wear characterization methods are all topics of active research [11-19].

AFM tip wear is used to understand fundamental wear mechanism at the nanoscale[14,20,21]. Although there are different tip failure mechanisms in AFM imaging, recent studies attribute tip wear at the nanoscale to atom-by-atom material removal from the asperity closest to the surface (Bhaskaran, et al.[14]), rather than Archand's wear law[22] (which describes macroscopic wear volume as being proportional to loading force and sliding distance). Gotmann and Lantz[20] proposed a model for wear analysis of single asperity sliding contact, where the material removal (breaking an atomic bond) is governed by the frictional stress acting on the contact. They established the wear rate by intermittently measuring the tip adhesion pull-off as a way to estimate the probe radius. Wear is determined by changes in probe tip-radius or volume using adhesion force measurements, blind reconstruction[23], electron microscope[24] or a combination [25].

One of the ways to develop robust AFM tips is to coat or fabricate them with materials that are resistant to wear[12]. The tribological properties of diamond-like carbon (DLC), such as resistance to abrasive and adhesive wear, low friction coefficient and high hardness [26,27], has made them a popular coating material for AFM tips [11,25,28-30].

### 1.1 CD-AFM Tip Wear

Most of the published work on AFM tip-wear has been on conventional AFMs rather than on critical dimension (CD) AFMs, which is used for niche applications in semiconductor manufacturing metrology. CD-AFM tips do not have a conical apex, rather they have a disk-like shape that is optimized for sidewall contact (Fig. 1a). So, unlike conventional AFM tips, the wear points for CD tips are at edges of this disk along the scan axis rather than at the vertical apex. In profile view, the disk-like part of the tip looks like a flare, and so these tips are usually referred to as flared tips. The few available studies show that silicon (Si) -based CD-AFM tips have relatively high wear rates that are unsuitable for accurate metrology[31,32]. Here, using a continuous scanning strategy, we evaluated the performance of electron beam deposited (EBD) and Si based CD tips with respect to tip-wear and tip lifetime, and present the results. We also propose a simple and unambiguous way to report wear-rate for CD-AFM tips. The focus of the paper is on methods for CD-AFM tip-wear comparisons rather than on the fundamental mechanism of CD-AFM tip-wear. However, the methods described here would be useful to researchers studying nanoscale sidewall wear mechanisms.

In CD-AFM, the scan algorithm dithers the tip in the lateral axis and vibrates it in the vertical axis[5,33,34]. For vertical or sidewall surfaces, a 2D adaptive scan algorithm[31,35,36] tracks the sample slope and continually adjusts the servo directions so the tip is in near-contact with the surface (Fig. 1). This allows the instrument to image sidewalls and re-entrant (undercut) features. Data are acquired based on sidewall morphology rather than a pre-specified scan rate. For top down measurements, the instrument works like a conventional AFM, but with lower lateral spatial resolution due to the relatively large flat bottom of CD tips relative to sharp conical tips. Due to the elongated nature of the tip and its close contact to the sidewall, the forces acting on the tip are distributed along the length of the tip that overlaps with the sidewall, rather than concentrated at the apex [37].

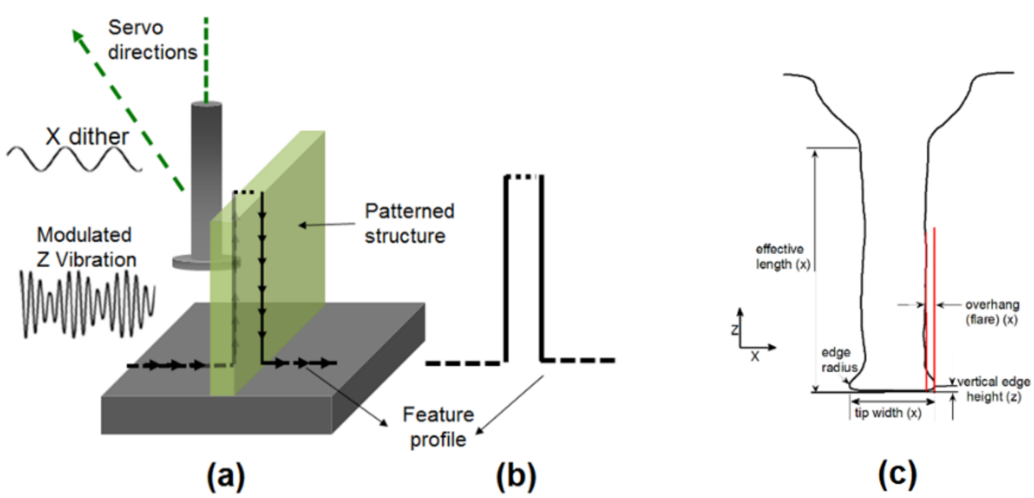


Fig. 1. Schematic diagram of CD-AFM operation. a) CD-AFM tip scanning a patterned feature. The tip vibrates in the Z direction and dithers in the lateral direction. b) Measured profile. The solid portions of the line indicate which segments of the profile were produced by the lateral apexes of the tip. C) Select CD-AFM tip parameters

tip flares and the sidewalls – which is the only time the tip flares interact with the surface. The wear points are thus the flares rather than the single vertical apex in conventional AFMs[38]. Wear calculations for CD-AFM tips should therefore account for the scan distance along the sidewalls. For example, in acquiring a line scan of 1μm that has a feature with a linewidth of 20 nm and a height of 100 nm, the CD-AFM lateral apexes would only come in "contact" with a length of 200 nm, the sum of the sidewalls on both sides of the feature. A conventional AFM tip would "contact" the surface for the full 1μm scan. Hence, a wear-parameter based on the total scan length would overestimate the relevant scan length (where the lateral apexes are in "contact" with the surface) and thus underestimate the wear rate. Definitions of wear such as those based on the number of sites are ambiguous if the actual sidewall contact is not clearly defined. The main advantage of calculating wear relative to sidewall travel is that it accounts for the relevant scan distance and makes it easier to compare tip-flare wear from images of features of different sizes. The method presented here differs from other AFM tip wear evaluation methods because we are only looking at the portions of the scan where the tip is in contact with the surface, which is appropriate for CD-AFM.

## 2. Materials and Methods

The parameters of interest are tip-width, wear rate and tip lifetime. Tip lifetime in our example is the total length of sidewall travel for each tip. Fig. 1c shows a profile of a CD-AFM tip, with select parameters. The tip-width is the most important parameter being monitored. Since accurate feature sizes are obtained by accounting for the tip-width, untracked changes in the tip-width would be manifested as apparent changes in feature sizes. Tip-flare determines the amount of reentrant feature the tip can measure. The vertical edge height (VEH) is the difference between the bottom of the tip and the flare apex (*z* direction) and causes an apparent shift in the location. of the bottom edge. For example, a VEH of 10 nm means that the tip will not capture the last 10 nm at the bottom of the feature. The effective length determines the deepest trench a tip can measure.

The EBD tips were produced using a multi-step electron beam deposition yielding high-density diamond-like carbon (DLC) material [32,39] and following well-established methods for nanofabrication of super sharp AFM probes[40,41]. In this process, an AFM cantilever is placed inside a low-pressure chamber containing carbonaceous precursors. The electron beam is then focused in a controlled manner to deposit tips of desired lengths, shapes and parameters. Figure 2 shows a transmission electron microscopy (TEM) image of a DLC CD-AFM tip with the overall structure of the tip, and the underlying conical tip.

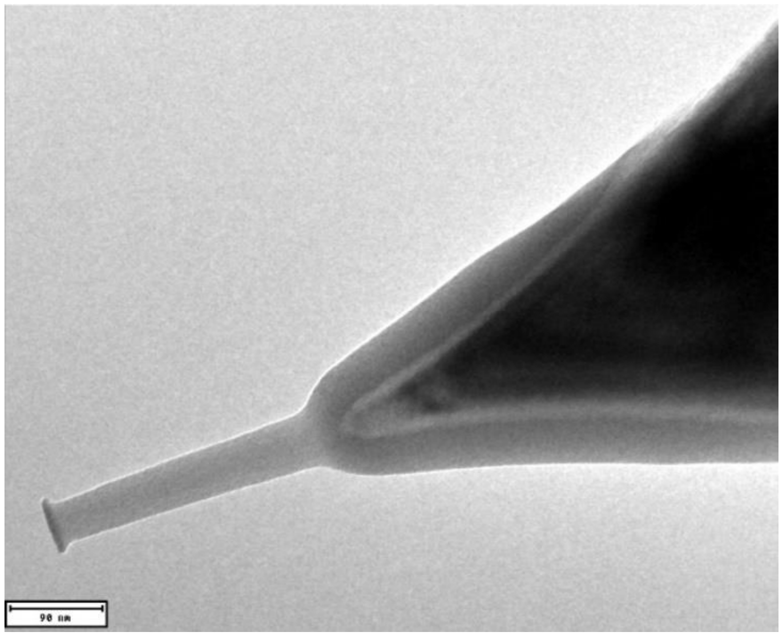

Figure 2: Representative TEM image of an DLC CD-AFM tip showing the e-beam deposited part of the tip and the underlying silicon conical tip.

The tip widths were characterized using a linewidth calibration sample[2] (NanoCD45®, VLSI Standards[a])[42] and NIST single-crystal CD reference material (SCCDRM)[43]. The tip shape was evaluated using a qualification procedure based on tangent slope and modified erosion (morphological operation) algorithms[44]. All the tips were nominally 50 nm in width.

[a] Certain commercial equipment, instruments, or materials are identified in this paper in order to specify the experimental procedure adequately. Such identification is not intended to imply recommendation or endorsement by the National Institute of Standards and Technology, nor is it intended to imply that the materials or equipment identified are necessarily the best available for the purpose.

The sample is an array of 3 etched Si lines with vertical and parallel sidewalls along the (111) plane, with nominal 115 nm linewidths with a spacing of 500 nm. The measurements were performed using a Veeco (Bruker) Insight® 3D-AFM.

Each tip evaluation starts with a calibration of tip width traceable to the SI meter. This is accomplished by measurement the apparent width of a working standard which has been referenced to the NIST SCCDRM calibration sample. This procedure is traceable to the SI meter with a combined uncertainty ($k$=2) of 0.8 nm and helps establish the initial tip size. Next we characterize the tip using size and shape characterization samples (IVPS and IFSR, Team Nanotec). Using a tangent slope and modified erosion (morphological operation) algorithm described in ref. [44], the tip-width, VEH, effective tip length, and tip profile are obtained. Next we measure two locations designated as monitor sites (explained later), and then the primary measurement site. Each image at the primary site is 1.8 μm × 500 nm and has 20 lines. For each scan line, both lateral tip apexes are in near contact with the sidewall for only 300 nm, which totals 6 μm per image. This is considerably less than the total lateral scan distance of 36 μm per image, which underscores the aforementioned importance of defining wear parameters relevant to CD-AFM. Each measurement is a separate tip-engage with the same settings. In each case, the scan location is identified by optical pattern recognition, the tip engages the surface, and scans reference features in both $x$ and $y$ axes and then the scanner offsets to the measurement location with respect to those features. This single tip-engage and feature pattern recognition for each measurement eliminates location drift between images. Tip-qualification measurements were made after every ten primary site measurements. To mitigate substrate or sample wear, we used a total of three primary measurement sites. This deviates from a lot of conventional wear measurement protocols, which calls for changing the scan location because of possible substrate wear. In our case, we wanted to see if there is sample wear after extended periods of measurement, so using more than one site was a good balance. In addition, our samples are features that are calibrated before use, rather than smooth surfaces, so it is easier to monitor and detect sample wear. The monitor sites were remeasured after every 500 primary site images. The measurement sequence ran until the tip was completely worn or failed catastrophically. In a few cases, the recipe was stopped, and a final tip width measurement was made relative to the SCCDRM calibration sample. The evaluation method (which did not include sliding contact as used in typical AFM tip wear tests) was chosen to best mimic actual measurements in an industrial setting. Also since CD-AFM implementation is based on “intermittent-contact,” the wear mechanism would be more representative of those obtained with intermittent contact mode AFM[29]. All measurements were acquired in a controlled environment with temperature and relative humidity stabilized to 20 °C ± 0.25 °C and 40% ± 5%, respectively. An overview of the measurement sequence is shown in fig. 3.

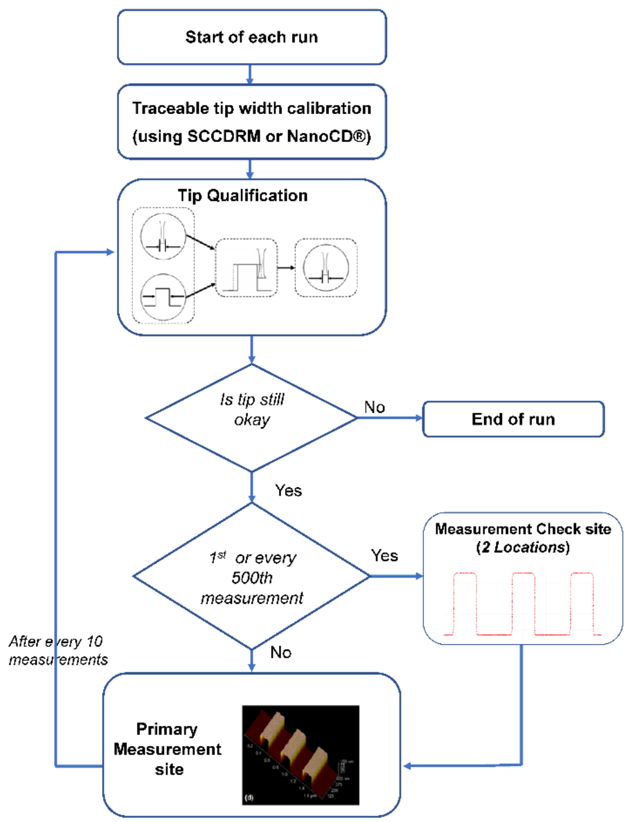


Figure 3: Overview of the measurement sequence.

## 3. Results

The tip-width results obtained from each of the tip-qualifications taken after every ten measurements are used to track the wear rate. Figure 4 shows select tip profiles taken at different intervals for Tip C, and the first and last profiles overlaid.

Figure 5 shows the tip-width data with respect to sidewall travel for all the tips used in the evaluation, and the per site wear rate for each tip. The sidewall travel length corresponds to the sum of sidewall travel in all the images taken with each tip. The sidewall length for each tip in Fig. 5 indicates the distance the test ran before the tip was either removed for further analysis or suffered catastrophic failure. Each millimeter of total sidewall travel corresponds to 164 measurements.

The wear rates are shown in Table 1. Linewidth results of the test features for each tip are shown in Table 2. Figure 6a and 6b show initial and final scanning electron microscopy (SEM) images for Tip A. The SEM images are used for visual quality check rather than quantitative analysis. Figure 6c has overlaid profiles of Tip A showing the initial profile and profiles after 2 mm and 13.04 mm of sidewall travel. A representative CD-AFM image from the test sample is shown in Fig. 6d.

## 4. Discussion

The data in Fig. 5 show that EBD tip lifetime was significantly longer due to reduced tip-wear compared to Si tips. This is based on the overall wear rate and the length of scan for each tip. Each EBD wear data exhibits a bilinear pattern that was not observed in the Si tips. In each case, the initial EBD tip wear-rate was always faster, but slowed down after about 2 mm of sidewall travel. In all cases the EBD tips showed less overall wear than the Si tips. Our hypothesis is that once the highest asperities wear out, the tip now has a larger surface area that is in contact with the sidewall, so the contact force is more distributed, resulting in a more gradual wear rate. This is consistent with explanations put forward by both Gotsmann and Lantz [20] and Liu et al[45] that as the tip becomes blunter and the contact area increases, the contact stress decrease and this leads to less wear. They posit that this will happen even as the overall load increases. In our case, we believe that the Si tips would have shown this trend if they scanned for a longer period of times before being destroyed. This should be the case since the tip/sample contact interactions are governed by the same contact model. What is clear from the data is that this inflexion point did not occur at a similar scan length as the EBD tips, resulting in a much faster wear rate for the Si tips. The catastrophic failure of the Si tips points to increased adhesion due to the larger contact area, which in turn increased the stiction between the Si tip and Si surface.

Although the total sidewall travel for each tip is different, this does not change the initial and extended wear rates shown in Table 1. The tip with the longest tip-lifetime (Tip C) measured a total of 3188 sites and has a wear rate of the 0.44 nm per millimeter of sidewall travel (0.0032 nm/site). This compares favorably with an earlier CD-AFM tip wear study by Liu, et al., where they obtained a wear rate of 0.0073 nm/site using Si tips coated with

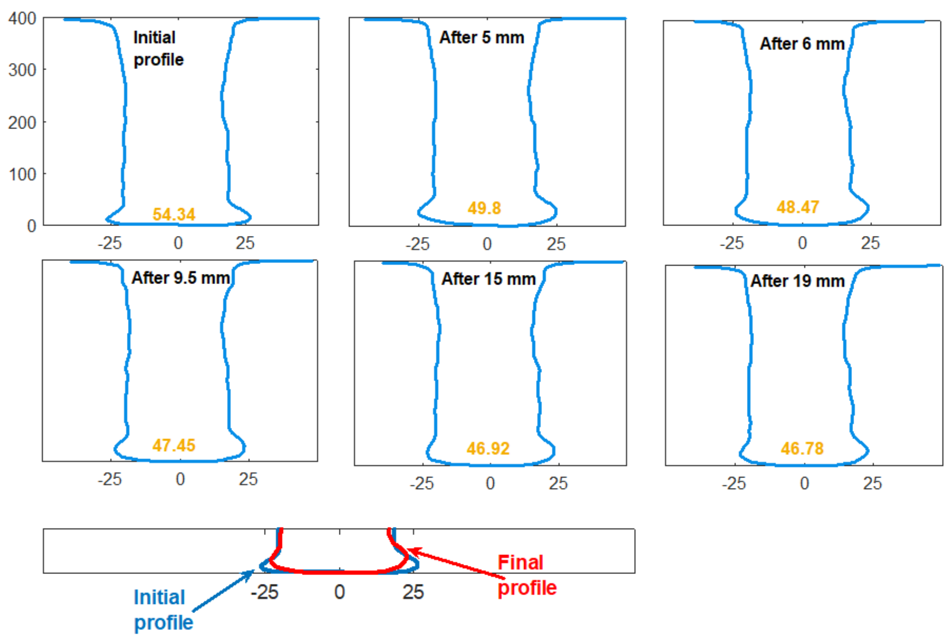


Figure 4: Selected tip profiles for Tip C from the intermittent tip qualification during the run obtained using tangent slope and modified erosion(morphological operation) algorithms described in ref. [44]. All the axes values are in nanometers. The y-axis scales are the same for all the plots.

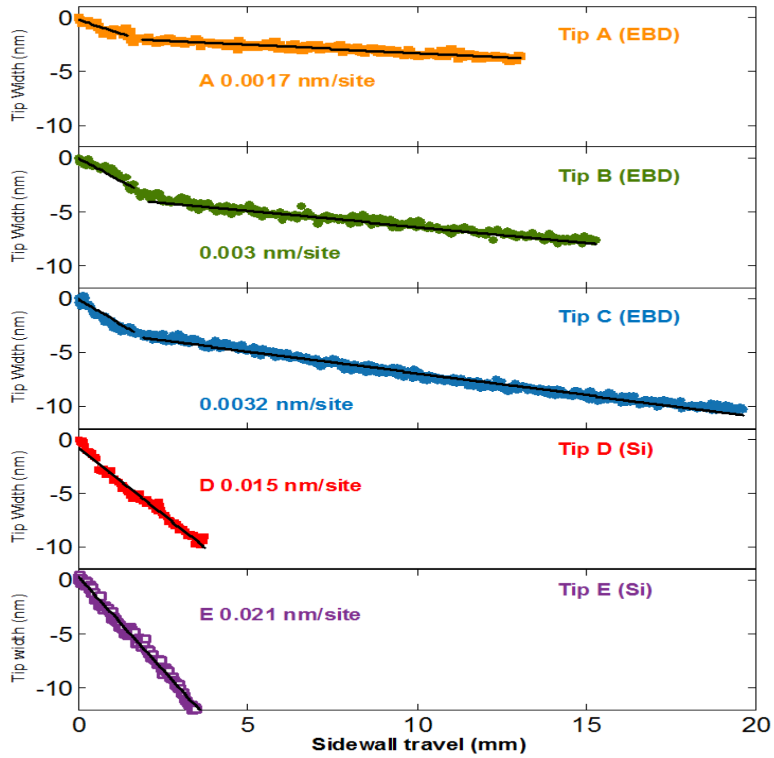


Fig. 5: Wear of EBD and *Si* tips used in the study. Each mm of sidewall travel represents 164 measurements (sites).

**Table 1** Wear rate for the different tips evaluated

| Tip | Wear (nm/mm of sidewall travel) | | |
|---|---|---|---|
| | Initial | Extended | Overall |
| A(EBD) | 0.99 | 0.15 | 0.2 |
| B(EBD) | 1.66 | 0.3 | 0.39 |
| C(EBD) | 1.87 | 0.4 | 0.44 |
| D(Si) | | | 2.55 |
| E (Si) | | | 3.5 |

**Table 2** Linewidth results of the test tips

| Tip | Linewidth Values (nm) | |
|---|---|---|
| | Mean | 1 Standard Deviation |
| A(EBD) | 114.0 | 0.59 |
| B(EBD) | 114.6 | 0.45 |
| C(EBD) | 114.4 | 0.52 |
| D(Si) | 114.2 | 0.61 |
| E (Si) | 114.9 | 0.41 |

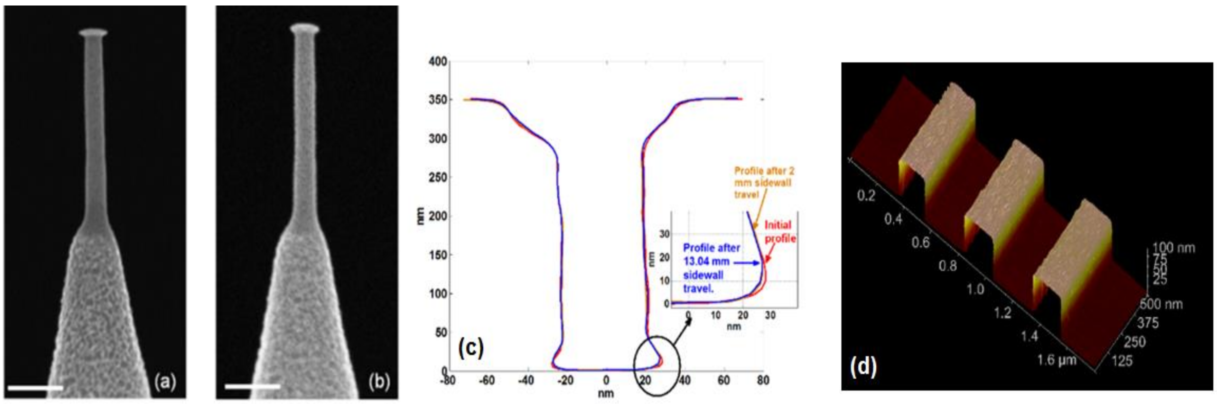


Figure 6. SEM images of Tip A a) Before use and b) after 13.04 mm (2139 measurement sites) of sidewall travel, showing minimal changes to the tip. The scale bar equals 100 nm. C) Overlaid profiles of tip A showing the initial profile, profile after 2 mm, and profile after 13.04 mm of sidewall travel. The profiles were obtained using tangent slope and modified erosion(morphological operation) algorithms described in ref. [44]. (d) Representative image from the test sample. Instrument: Insight CD-AFM, scan size: x:1.8 μm, y: 500 nm; z-range: 100. Tip: CD-AFM EBD; average scan speed:0.477Hz. Image includes the effect of tip dilation.

hydrophobic self-assembled monolayers. Since the prior work did not specify the sidewall scan length of each site, only the final wear per site values are being compared. This underscores the value of using sidewall travel length to evaluate the data. Overall the tip lifetime of the EBD tips was at least double that of the Si tips, consistent with the prior findings of Liu et al.[31] and Foucher et al.[32]

The reduced wear for the EBD tips is attributed to hardness of the EBD DLC material [26,27,46] and reduced adhesion between the Si features and the hydrogenated amorphous carbon (a-C:H) material of DLC. This difference in adhesion also complicates long term studies of Si tips because these are more likely to fail catastrophically due to adhesion induced stiction, a known failure mechanism for NEMS/MEMS[46]. Just 10 nm of tip wear could erode the flares such that the tip would no longer be capable of re-entrant imaging. This also constraints tip lifetime.

Although the results shown in Fig. 5 indicate different tip lifetimes, it is important to note that the linewidth results were consistent. As shown in Table 2, the linewidth values do not correlate to differences in wear rate. The tip-qualification[44] component of CD-AFM, where the tip-width is measured before each measurement or at specified intervals, ensures that the width information is monitored.

### 4.1 Uncertainty Considerations

The wear rate values shown in table 1 are based on tip-widths obtained intermittently during the scan, as described in section 2. Hence, the uncertainty of these values is based on the uncertainty of the tip-width determination $\underline{u}_{\mathrm{Tip}} = ((tip_{\mathrm{zeroth\_order}})^2 + (e_{HO\_1})^2)^{1/2}$ (described in detail in refs. [33,43,47]), where $tip_{\mathrm{zeroth\_order}}$ is the size uncertainty component and $e_{HO\_1}$ is the shape uncertainty component. $tip_{\mathrm{zeroth\_order}}$ comes from applying a constant offset to correct for tip dilation and includes contributions from the transmission electron microscopy (TEM) calibration and the calibration transfer process. $e_{HO\_1}$, (also referred to as higher order tip effects), are shape dependent errors and are sometimes included as part of the repeatability estimate. Note that the values given by $\underline{u}_{\mathrm{Tip}}$ describes the uncertainty relative to the SI (*Système International d'Unites* or International System of Units) meter, since the $tip_{\mathrm{zeroth\_order}}$ includes values from TEM lattice counting calibration[8,48].

A potential source of uncertainty is positioning errors during tip-width determination. The portion of the IVPS used for tip qualification is aided by optical and profile scan pattern recognition of fiducials near the site. This ensures that positioning errors are not from the large range positioning-stage, but by the linearity of the *x-y* scanner, which in our case is approximately 0.01% or lower. In addition, the IVPS tip-width determination site is not a single location, but rather covers a measurement window, so the tip is not required to land on the exact same spot for the measurements to be valid. Hence, the positioning errors will be captured as part of the statistical variation (Type A)[49] of the measurement.

Another source of uncertainty is the potential wear of the tip-width determination site. Given the large number of measurements at the tip-width qualification site, there is a possibility that this location could gradually wear, and such wear would go undetected. The monitor sites mentioned in the methods section is used to detect if this is happening. If there is no wear at the tip-qualification site, the values obtained from the monitor site should be consistent throughout the run. If the features at the site are wearing, the calculated tip-width will be larger and the values from the monitor site will gradually decrease. This was not the case. The differences in the monitor site values were random and less than 0.5 nm, well below the uncertainty of the measurement and indicates that that there was no wear of the tip-qualification site. Since the difference in the monitor-site values is used to determine if the data is useful, we estimated an uncertainty for it. The model for this potential uncertainty is $u_{measurement\_check} = \left[\frac{(LW_{diff})}{2}\right]/\sqrt{3}$ where $LW_{diff}$ is the largest difference in the monitor-site values, and using a rectangular distribution with $(LW_{low}/2)_-$ and $(LW_{high}/2)_+$ as the bounds of the distribution. This is a relatively conservative estimate, but one that is warranted by the "go" and "no go" importance of the monitor-site values. Our use of two monitor sites was a precaution against possible sample damage or tip crashes. Our estimate of the tip-width uncertainty is 0.95 nm (*k*=1) [43].

## 5. Conclusion

Wear and tip lifetime of CD-AFM EBD tips were evaluated. Observed wear rates ranged from approximately 8 to 17 times lower than those of Si based CD-AFM tips. We also used a sidewall scan length approach to defining wear rates. This essentially means normalizing the wear rate to the portions of the scan that comes in contact with the feature sidewall. The lower wear and greater lifetime of DLC EBD tips relative to Si tips is attributed to hardness of the DLC material and lower adhesion between the DLC tip material and the Si sidewalls, as compared with Si-Si contact for Si tips. Lower wear rate leads to less variability; and the ability to develop tips with reduced adhesion to the sample material will improve measurement reproducibility. We plan to extend this work to smaller tip sizes, additional tip parameters, DLC coated tips, additional tip and sample material, and the fundamental mechanism for this type of sidewall wear.

## *References*


[1] N.G. Orji, et al., Metrology for the next generation of semiconductor devices. *Nature Electronics*, **1**(10), 532 (2018), https://doi.org/10.1038/s41928-018-0150-9

[2] N.G. Orji, et al., 3D-AFM Measurements for Semiconductor Structures and Devices, in *Metrology and Diagnostic Techniques for Nanoelectronics*. Ma Z. and D.G. Seiler, Editors., Pan Stanford, New York:. (2017).

[3] D. Hussain, et al., Advances in the atomic force microscopy for critical dimension metrology. *Measurement Science and Technology*, **28**(1), 012001 (2016), http://dx.doi.org/10.1088/0957-0233/28/1/012001

[4] R. Kizu, et al., Development of a metrological atomic force microscope with a tip-tilting mechanism for 3D nanometrology. *Measurement Science and Technology*, **29**(7), 075005 (2018), https://doi.org/10.1088/1361-6501/aabe1a

[5] Y. Martin, et al., Method for imaging sidewalls by atomic force microscopy. *Applied Physics Letters*, **64**(19), 2498 (1994), https://aip.scitation.org/doi/abs/10.1063/1.111578

[6] R. Dixson, et al., Multilaboratory comparison of traceable atomic force microscope measurements of a 70-nm grating pitch standard. *J. of Micro/Nanolithography, MEMS, and MOEMS*, **10**(1), 013015 (2011), https://doi.org/10.1117/1.3549914

[7] N.G. Orji, et al., Progress on implementation of a reference measurement system based on a critical-dimension atomic force microscope. *J. of Micro/Nanolithography, MEMS, and MOEMS*, **6**(2), 023002 (2007), https://doi.org/10.1117/1.2728742

[8] G. Dai, et al., Comparison of line width calibration using critical dimension atomic force microscopes between PTB and NIST. *Measurement Science and Technology*, **28**(6), 065010 (2017), http://dx.doi.org/10.1088/1361-6501/aa665b

[9] A. Yacoot, et al., Aspects of scanning force microscope probes and their effects on dimensional measurement. *Journal of Physics D: Applied Physics*, **41**(10), 103001 (2008), http://dx.doi.org/10.1088/0022-3727/41/10/103001

[10] A. Vaid, et al., Hybrid metrology: from the lab into the fab. *J. of Micro/Nanolithography, MEMS, and MOEMS*, **13**(4), 041410 (2014), https://doi.org/10.1117/1.JMM.13.4.041410

[11] J. Liu, et al., Tribochemical Wear of Diamond-Like Carbon-Coated Atomic Force Microscope Tips. *ACS Applied Materials & Interfaces*, **9**(40), 35341 (2017), https://doi.org/10.1021/acsami.7b08026

[12] M.A. Lantz, et al., Wear-Resistant Nanoscale Silicon Carbide Tips for Scanning Probe Applications. *Advanced Functional Materials*, **22**(8), 1639 (2012), https://onlinelibrary.wiley.com/doi/abs/10.1002/adfm.201102383

[13] M. Rashidi, et al., Autonomous Scanning Probe Microscopy in Situ Tip Conditioning through Machine Learning. *ACS Nano*, **12**(6), 5185 (2018), https://doi.org/10.1021/acsnano.8b02208

[14] H. Bhaskaran, et al., Ultralow nanoscale wear through atom-by-atom attrition in silicon-containing diamond-like carbon. *Nat Nanotechnol*, **5**(3), 181 (2010), https://doi.org/10.1038/Nnano.2010.3

[15] J.P. Killgore, et al., Continuous Measurement of Atomic Force Microscope Tip Wear by Contact Resonance Force Microscopy. *Small*, **7**(8), 1018 (2011), https://doi.org/10.1002/smll.201002116

[16] E.E. Flater, et al., A simple atomic force microscope-based method for quantifying wear of sliding probes. *Review of Scientific Instruments*, **89**(11), 113708 (2018), https://aip.scitation.org/doi/abs/10.1063/1.5048584

[17] P. Zhang, et al., Comparison of wear methods at nanoscale: line scanning and area scanning. *Wear*, **400-401**, 137 (2018), https://doi.org/10.1016/j.wear.2018.01.004

[18] B. Park, et al. Application of carbon nanotube probes in a critical dimension atomic force microscope. *Proc. SPIE* **6518**, 651819 (2007), https://doi.org/10.1117/12.712326

[19] J. Choi, et al., Evaluation of carbon nanotube probes in critical dimension atomic force microscopes. *J. of Micro/Nanolithography, MEMS, and MOEMS*, **15**(3), 034005 (2016), https://doi.org/10.1117/1.Jmm.15.3.034005

[20] B. Gotsmann, et al., Atomistic Wear in a Single Asperity Sliding Contact. *Physical Review Letters*, **101**(12), 125501 (2008), https://link.aps.org/doi/10.1103/PhysRevLett.101.125501

[21] J.J. Liu, et al., *Proceedings of the Stle/Asme International Joint Tribology Conference 2008*, 37 (2009), https://doi.org/10.1115/IJTC2008-71135

[22] J.F. Archard, Contact and Rubbing of Flat Surfaces. *Journal of Applied Physics*, **24**(8), 981 (1953), https://aip.scitation.org/doi/abs/10.1063/1.1721448

[23] J.S. Villarrubia, Algorithms for scanned probe microscope image simulation, surface reconstruction, and tip estimation. *J Res Natl Inst Stan*, **102**(4), 425 (1997), https://doi.org/10.6028/jres.102.030

[24] T.D. Jacobs, et al., Characterizing nanoscale scanning probes using electron microscopy: A novel fixture and a practical guide. *Review of Scientific Instruments*, **87**(1), 013703 (2016), https://doi.org/10.1063/1.4937810

[25] T. Strahlendorff, et al., Tip wear and tip breakage in high-speed atomic force microscopes. *Ultramicroscopy*, **201**, 28 (2019), http://www.sciencedirect.com/science/article/pii/S0304399118301797

[26] J. Robertson, Diamond-like amorphous carbon. *Materials Science and Engineering: R: Reports*, **37**(4), 129 (2002), http://www.sciencedirect.com/science/article/pii/S0927796X02000050

[27] Y. Gogotsi, et al., Conversion of silicon carbide to crystalline diamond-structured carbon at ambient pressure. *Nature*, **411**(6835), 283 (2001), https://doi.org/10.1038/35077031

[28] J. Foucher, et al. Overcoming silicon limitations: new 3D-AFM carbon tips with constantly high resolution for sub-28 nm node semiconductor requirements. *Proc. SPIE* **8324**, (2012)

[29] V. Vahdat, et al., Atomic-Scale Wear of Amorphous Hydrogenated Carbon during Intermittent Contact: A Combined Study Using Experiment, Simulation, and Theory. *ACS Nano*, **8**(7), 7027 (2014), https://doi.org/10.1021/nn501896e

[30] G. Jänchen, et al., Mechanical properties of high-aspect-ratio atomic-force microscope tips. *Applied physics letters*, **80**(24), 4623 (2002), https://doi.org/10.1063/1.1485307

[31] H. Liu, et al., Advanced atomic force microscopy probes: Wear resistant designs. *J. Vac Sci Technol B*, **23**(6), 3090 (2005), https://doi.org/10.1116/1.2127936

[32] J. Foucher, et al. Development of a comprehensive metrology platform dedicated to dimensional measurements of CD atomic force microscopy tips. *Proc. SPIE* **9424**, (2015) 86811I

[33] R. Dixson, et al., Interactions of higher order tip effects in critical dimension-AFM linewidth metrology. *J. Vac Sci Technol B*, **33**(3), 031806 (2015), https://doi.org/10.1116/1.4919090

[34] R. Dixson, et al., Spatial dimensions in atomic force microscopy: Instruments, effects, and measurements. *Ultramicroscopy*, **194**, 199 (2018), https://doi.org/10.1016/j.ultramic.2018.08.011

[35] H.-C. Liu, et al., Critical Dimension Atomic Force Microscopy for Sub-50-nm Microelectronics Technology Nodes, in *Applied Scanning Probe Methods VIII*. Bhushan B., H. Fuchs, and M. Tomitori, Editors., Springer, Heidelberg. (2008).

[36] N.G. Orji, et al., Tip characterization method using multi-feature characterizer for CD-AFM. *Ultramicroscopy*, **162**, 25 (2016), http://dx.doi.org/10.1016/j.ultramic.2015.12.003

[37] V.A. Ukraintsev, et al., Distributed force probe bending model of critical dimension atomic force microscopy bias. *J. of Micro/Nanolithography, MEMS, and MOEMS*, **12**(2), 023009 (2013), https://doi.org/10.1117/1.JMM.12.2.023009

[38] R.G. Dixson, et al., Multiple-instrument evaluation of the consistency and long-term stability of tip width calibration for critical dimension atomic force microscopy. *J. of Micro/Nanolithography, MEMS, and MOEMS*, **16**(2), 024003 (2017), https://doi.org/10.1117/1.JMM.16.2.024003

[39] S.W. Schmidt, et al. Controlled fabrication of advanced functional structures on the nanoscale by means of electron beam-induced processing. *Proc. SPIE* **8763**, 876316 (2013), https://doi.org/10.1117/12.2017430

[40] I. Utke, et al., Gas-assisted focused electron beam and ion beam processing and fabrication. *Journal of Vacuum Science & Technology B: Microelectronics and Nanometer Structures Processing, Measurement, and Phenomena*, **26**(4), 1197 (2008), https://doi.org/10.1116/1.2955728

[41] M. Wendel, et al., Sharpened electron beam deposited tips for high resolution atomic force microscope lithography and imaging. *Applied physics letters*, **67**(25), 3732 (1995), https://doi.org/10.1063/1.115365

[42] M. Tortonese, et al. Sub-50 nm isolated line and trench width artifacts for CD metrology. *Proc. SPIE* **5375**, 647 (2004), https://doi.org/10.1117/12.536812

[43] N.G. Orji, et al. TEM calibration methods for critical dimension standards. *Proc. SPIE* **6518**, 651810 (2007), https://doi.org/10.1117/12.713368

[44] G. Dahlen, et al., Tip characterization and surface reconstruction of complex structures with critical dimension atomic force microscopy. *J. Vac Sci Technol B*, **23**(6), 2297 (2005), https://doi.org/10.1116/1.2101601

[45] J.J. Liu, et al., Method for Characterizing Nanoscale Wear of Atomic Force Microscope Tips. *Acs Nano*, **4**(7), 3763 (2010), https://doi.org/10.1021/nn100246g

[46] B. Bhushan, Adhesion and stiction: Mechanisms, measurement techniques, and methods for reduction. *Journal of Vacuum Science & Technology B: Microelectronics and Nanometer Structures Processing, Measurement, and Phenomena*, **21**(6), 2262 (2003), https://avs.scitation.org/doi/abs/10.1116/1.1627336

[47] N.G. Orji, et al., Higher order tip effects in traceable CD-AFM-based linewidth measurements. *Measurement Science and Technology*, **18**(2), 448 (2007), https://doi.org/10.1088/0957-0233/18/2/S17

[48] N.G. Orji, et al. Measurement traceability and quality assurance in a nanomanufacturing environment. *Proc. SPIE* **7405**, 740505 (2009), https://doi.org/10.1117/12.826606

[49] B.N. Taylor, et al., Guidelines for evaluating and expressing the uncertainty of NIST measurement results. *NIST Tech. Note 1297*, (1994),

# Preprint.

***See published version at:*** N. G. Orji, R. G. Dixson, E. Lopez, and B. Irmer "Wear comparison of critical dimension-atomic force microscopy tips," *J. of Micro/Nanolithography, MEMS, and MOEMS* 19(1), 014004 (2020). https://doi.org/10.1117/1.JMM.19.1.014004